7-29-2005

A role for mitogen-activated protein kinase (Erk1/2) activation and non-selective pore formation in P2X7 receptor-mediated thymocyte death

Rodolphe Auger
Université Paris-Sud

Iris Motta
Université Paris

Karim Benihoud
Université Paris-Sud

David M. Ojcius
University of California, Merced, dojcius@pacific.edu

Jean M. Kanellopoulos
Université Paris-Sud, Jean.Kanellopoulos@ibbmc.u-psud.fr

A Role for Mitogen-activated Protein Kinase[Erk1/2] Activation and Non-selective Pore Formation in P2X7 Receptor-mediated Thymocyte Death*

Rodolphe Auger‡, Iris Motta‡, Karim Benihoud‡, David M. Ojcius§, and Jean M. Kanellopoulos‡¶

From the ‡Institut de Biochimie et Biophysique Moléculaire et Cellulaire, Université Paris-Sud, 91405 Orsay cedex, France and the §School of Natural Sciences, University of California, Merced, California 95344

Extracellular ATP (ATPe) binds to P2X7 receptors (P2X7R) expressed on the surface of cells of hematopoietic lineage, including murine thymocytes. Activation of P2X7R by ATPe results in the opening of cation-specific channels, and prolonged ATPe exposure leads to the formation of non-selective pores enabling transmembrane passage of solutes up to 900 Da. In the presence of ATPe, P2X7R-mediated thymocyte death is due primarily to necrosis/lysis and not apoptosis, as measured by the release of lactate dehydrogenase indicative of a loss of plasma membrane integrity. The present study is focused on the identification of P2X7R signaling mediators in ATP-induced thymocyte necrosis/lysis. Thus, extracellular signal-regulated protein kinase 1/2 (Erk1/2) phosphorylation was found to be required for cell lysis, and both events were independent of ATP-induced calcium influx. P2X7R-dependent thymocyte death involved the chronological activation of Src family tyrosine kinase(s), phosphatidylinositol 3-kinase, the mitogen-activated protein (MAP) kinase[Erk1/2] module, and the proteasome. Although independent of this signaling cascade, non-selective pore formation may modulate ATP-mediated thymocyte death. These results therefore suggest a role for both activation of MAP kinase[Erk1/2] and non-selective pore opening in P2X7R-induced thymocyte death.

Extracellular ATP interacts with P2 purinergic receptors that are expressed on a wide spectrum of tissues. Two classes of P2 receptors have been identified, the G-protein-coupled seven-transmembrane P2Y receptors and the P2X ligand-gated cation channels (1). Seven members of the P2X receptor family have been cloned, which share the same predicted structure with two transmembrane-spanning domains, an extracellular loop and intracellular N- and C-terminal tails. The P2X7 receptor (P2X7R)[1] differs from the other P2X receptors; in particular, its C-terminal domain is 200 amino acids longer and it does not heteropolymerize with other members of the P2X family (2). Brief exposure to millimolar concentrations of ATP in its fully dissociated tetra-anionic form, ATP^{4-}, opens cation-specific ion channels. Prolonged triggering of P2X7R results in the formation of non-selective membrane pores permeable to molecules of molecular mass up to 900 Da. Formation of the non-selective pore is dependent on the cytoplasmic C-terminal domain of P2X7R (3–5). However, it is still unclear whether it results from dilatation of the P2X7R-induced cation channel or from interaction of P2X7R with a distinct channel protein, which allows the entry of larger molecules (reviewed in Ref. 6).

Depending on the cell type, numerous physiological functions have been attributed to P2X7R; notably, formation of giant cells (7, 8), activation of caspase 1 (9, 10), and rapid release of mature interleukin-1β from macrophages (11, 12), shedding of membrane molecules such as L-selectin (13, 14) and CD23 (13), and killing of various intracellular pathogens in macrophages (15–17).

In most cells that express the P2X7R, sustained stimulation with ATP leads to membrane blebbing and cell death (18, 19). In particular, cell death has been observed in different cells of hematopoietic origin such as lymphocytes (20), thymocytes (21, 22), macrophages (23, 24), and dendritic cells (25, 26). The physiological significance of cell death mediated by the ligation of P2X7R by ATP remains to be determined. A potential role for ATP in programmed cell death underlying positive and negative selection of immature thymocytes during thymus development has been suggested by Chvatchko *et al.* (27). In *in vitro* dexamethasone- or *in vivo* superantigen-induced apoptosis, P2X1R is up-regulated and P2X1R antagonists inhibit thymocyte death, suggesting that the elimination of self-reactive thymocytes may be mediated by the P2X1R (27). On the other hand, death by neglect may be due to one or more pyridoxal-phosphate-6-azophenyl-2′,4′-disulfonic acid-sensitive receptors, *i.e.* P2X1R, -2R, and/or -7R (28). However, the role of P2X1R in negative selection has been challenged by Koshiba *et al.* (29), who reported that mouse thymocytes treated with dexamethasone or anti-CD3 mAb respond by up-regulating P2Y2R mRNA expression but not modifying P2X1R mRNA transcripts. Thus, the potential role of ATP in programmed cell death in the thymus still remains elusive.

P2X7R stimulation triggers several intracellular signaling pathways. Thus, in macrophages (30) and thymocytes (31), calcium-dependent phospholipase D activation is observed, but this enzymatic activity is not involved in cell death. The role of

[1] The abbreviations used are: P2X7R, P2X7 receptor; MAP, mitogen-activated protein; Erk, extracellular-signal regulated kinase; JNK, c-Jun N-terminal kinase; PI3K, phosphatidylinositol 3-kinase; PI4K, phosphatidylinositol 4-kinase; o-ATP, oxidized ATP; LDH, lactate dehydrogenase; AMC, 7-amino-4-methylcoumarin; PP2, 4-amino-5-(4-chlorophenyl)-7-(*t*-butyl)pyrazolo[3,4-*d*]pyrimidine; PARP, poly(ADP-ribose) polymerase; HMGB1, high-mobility group box 1 protein; MEK, MAP kinase kinase; mAb, monoclonal antibody.

P2X7R in controlling protein kinase activities (32–34), the generation of superoxide (35), as well as activation of transcriptional factors (36, 37) has been tested in various cellular models. However, the relationship between these biochemical events and cell death has not been fully characterized. A role for caspase-1 in P2X7R-mediated cell death has been established for macrophages stimulated by lipopolysaccharide. In this model, brief exposure of macrophages to ATP leads to death by two different pathways, one of which is lipopolysaccharide-independent, and the other, lipopolysaccharide-induced and requiring caspase-1 (24).

In murine thymocytes, P2X7R activation by ATP leads to death via both caspase-dependent apoptosis, albeit a minor component of cells dying, and, predominantly, via necrosis/lysis (31), but the mechanisms of death have not been elucidated. We therefore focused our study on the intracellular signaling events occurring during thymocyte death following *in vitro* ATP treatment. We show that stimulation of P2X7R in thymocytes induces the activation of the three mitogen-activated protein (MAP) kinase modules, extracellular-signal regulated kinases 1/2 (Erk1/2), c-Jun N-terminal kinases 1/2 (JNK1/2), and p38 kinases. However, only the MAP kinase$^{Erk1/2}$ module is necessary for calcium-independent necrosis/lysis of thymocytes. Using specific inhibitors of various enzymes, we determined that thymocyte death requires the sequential activation of one or more Src family tyrosine kinases, phosphatidylinositol 3-kinase (PI3K), the extracellular signal-regulated kinases 1/2, and the proteasome. Formation of the non-selective pore is independent of this signaling pathway, and in particular, of the activation of the MAP kinase$^{Erk1/2}$ module, but both pore formation and the signaling pathway contribute to thymocyte death.

MATERIALS AND METHODS

Animals—Four- to eight-week-old C57BL/6 and BALB/c mice were purchased from Charles River Laboratories. P2X7R-deficient C57BL/6 mice were obtained from Pfizer Inc.

Reagents—ATP, dexamethasone, oxidized ATP (o-ATP), and lactate dehydrogenase (LDH) detection kits were purchased from Sigma. Rapamycin, phorbol 12-myristate 13-acetate, genistein, 4-amino-5-(4-chlorophenyl)-7-(*t*-butyl)pyrazolo[3,4-*d*]pyrimidine (PP2), wortmannin, LY294002, okadaic acid, U0124, U0126, SB 203580, SP 600125, anisomycin, lactacystin, cycloheximide, actinomycin D, and the fluorogenic peptide substrate, Suc-Leu-Leu-Val-Tyr-AMC, were purchased from Calbiochem. EtBr and all cell culture media reagents, except RPMI 1640 without calcium, were obtained from Invitrogen. RPMI 1640 without calcium was purchased from BIO MEDIA. YO-PRO-1 iodide was from Molecular Probes. All other reagents were obtained from Sigma.

Antibodies—The following antibodies were used for immunoprecipitation or Western blotting: unconjugated rabbit anti-Erk1/2 (pTpY185/187), anti-JNK1/2 SAPK(pTpY183/185), anti-p38 (pTpY180/182), anti-Src (pY418) phosphospecific antibodies (BIOSOURCE International), rabbit anti-Akt (pS473) antibody (Cell Signaling), goat anti-actin (I-19), rabbit anti-Erk1/2 (Zymed Laboratories Inc.), rabbit anti-p38 (C20), rabbit anti-c-Src (SRC2), goat anti-Akt1, mouse monoclonal anti-Lck (3A5), mouse monoclonal anti-Fyn (15) antibodies (Santa Cruz Biotechnology), mouse mAb anti-poly(ADP-ribose) polymerase (PARP) (Ab-2, Oncogene Research Products), affinity-purified rabbit anti-high mobility group box 1 (HMGB1) antibody (BD Pharmingen), affinity-purified rabbit anti-C-terminal region of rat P2X7R (Alomone Laboratories). Affinity-purified goat anti-Rabbit IgG coupled to peroxidase (Rockland Immunochemicals)-, goat anti-mouse IgG-coupled to peroxidase-, and mouse monoclonal anti-goat/sheep IgG-peroxidase-conjugated antibodies (Sigma-Aldrich) were used as secondary antibodies for Western blot analyses.

Measurement of LDH Release—In most experiments, mouse thymocytes were preincubated in culture medium without fetal calf serum for 1 h with inhibitors, unless otherwise specified in the figure legends, before addition of 1 mM ATP for 2 h. Cell lysis was quantified by measuring the release of LDH or HMGB1. Mouse thymocytes (5×10^6) were incubated in 0.5 ml RPMI containing 1 mg/ml of bovine serum albumin at 37 °C for various lengths of time. Cells were centrifuged at

$200 \times g$ for 10 min, and supernatants were tested for LDH release using the oxidation reaction of β-NADH in the presence of pyruvate (Sigma kit for LDH). The initial rate of absorbance decrease was measured in an automatic readout spectrophotometer at $\lambda = 340$ nm (38).

Immunoprecipitation—Ten million thymocytes were lysed in 0.2 ml of lysis buffer containing 50 mM phosphate buffer, pH 7.4, 0.15 M NaCl, 1% Triton X-100, 5 mM EDTA, 30 mM sodium pyrophosphate, 50 mM sodium fluoride, 30 mM sodium pervanadate, at 4 °C. Cells were incubated 30 min on ice. Lysates were centrifuged at $12,000 \times g$ for 15 min at 4 °C. Equal amounts of cell lysates were incubated overnight with anti-Lck or anti-Fyn at 2 μg/ml. To precipitate immune complexes, Protein-G-Sepharose was added for 2 h. Immune complexes bound to Protein-G-Sepharose were washed three times and resuspended in loading buffer containing β-mercaptoethanol.

Western Blot Analyses—Lysates or immunoprecipitates from mouse thymocytes were analyzed by SDS-PAGE and transferred to nitrocellulose membranes, which were blocked with 3% nonfat milk in Tris-buffered saline containing 0.2% Tween 20 for 1 h at 37 °C. Blots were immunostained with primary antibodies at 4 °C overnight and probed with secondary antibodies conjugated to horseradish peroxidase. Specific bands were visualized by enhanced chemiluminescence (PerkinElmer Life Sciences).

Analysis of Proteasome Activity—To measure proteasome activity in intact thymocytes, 2.5×10^6 cells were suspended in 100 μl of phosphate-buffered saline containing 20 μM D-glucose and 1 mg/ml bovine serum albumin in a flat bottom 96-well plate. Cells were incubated or not with inhibitors for 1 h at 37 °C and treated with 1 mM ATP for 2 h. The fluorogenic peptide substrate for chymotrypsin-like proteasome activity, Suc-Leu-Leu-Val-Tyr-AMC, was then added at 20 μM, and the plate was incubated at 37 °C for an additional 2 h. Substrate conversion was measured with a spectrofluorometer (Wallac 1420), using an excitation wavelength of 390 nm, and measuring fluorescence at an emission wavelength of 460 nm.

Non-selective Pore Formation—Thymocytes were incubated 15 min at 37 °C in the presence of ATP (1 mM) and YO-PRO-1 (2 μM) in assay buffer containing 280 mM sucrose, 10 mM HEPES (pH 7.4), 5 mM *N*-methyl-D-glucamine, 5.6 mM KCl, 10 mM D-glucose, 1 mM CaCl$_2$ (39). Cells were pelleted for 10 min at $200 \times g$ and incubated with propidium iodide (0.5 μg/ml) in assay buffer at 4 °C. Cell suspensions were then analyzed by flow cytometry.

For EtBr uptake experiments, 2.5×10^6 thymocytes were suspended in 100 μl of the same assay buffer containing 10 μg/ml ethidium bromide in a flat bottom 96-well plate. ATP (1 mM) was added, and fluorescence was monitored for 40 min at 37 °C in the spectrofluorometer using an excitation wavelength of 485 nm and an emission wavelength of 615 nm.

Real-time PCR Assays—Briefly, 2 μg of total RNA, extracted from thymocytes using TRIzol reagent (Invitrogen), were reverse-transcribed using SuperScript First-Strand Synthesis system for reverse transcription-PCR (Invitrogen). The quantitative real-time PCR reactions were performed using LightCycler FastStart DNA Master^{Plus} SYBR Green I mix (Roche Applied Science) in a LightCycler 2.0 (Roche Applied Science). P2X7R RNA expression data were normalized to that of actin. The following mouse P2X7R and actin primers were used: P2X7R forward, 5′-TTCCAGGAAGCAGGAGAGAA-3′; P2X7R reverse, 5′-ATAC-TTCAACGTCGGCTTGG-3′; actin forward, 5′-GCTACAGCTTCACCA-CCACA-3′; actin reverse, 5′-AAGGAAGGCTGGAAAAGAGC-3′.

RESULTS

ATP-induced Thymocyte Death—ATP-treated thymocytes undergo cell lysis and apoptosis, as assessed, respectively, by the release of cytosolic lactate dehydrogenase (LDH) (Fig. 1*A*) (31) and caspase-dependent DNA fragmentation (31). To further elucidate the basis for cell lysis, we took advantage of two assays that discriminate between the two types of cell death, namely, the release of HMGB1, a chromatin-associated nuclear protein that is liberated into the cytosol of necrotic but not apoptotic cells (40); and the cleavage of PARP, a nuclear protein that is a specific substrate of caspase-3 and is an indicator of apoptotic cell death. We thus determined the kinetics of these two events in thymocytes exposed to an optimal dose of ATP. As can be seen in Fig. 1*B*, HMGB1 is detected as early as 2 h following ATP stimulation, and increases until 5 h of culture. In comparison, dexamethasone, a known apoptotic agent for thymocytes, induces a significantly reduced level of
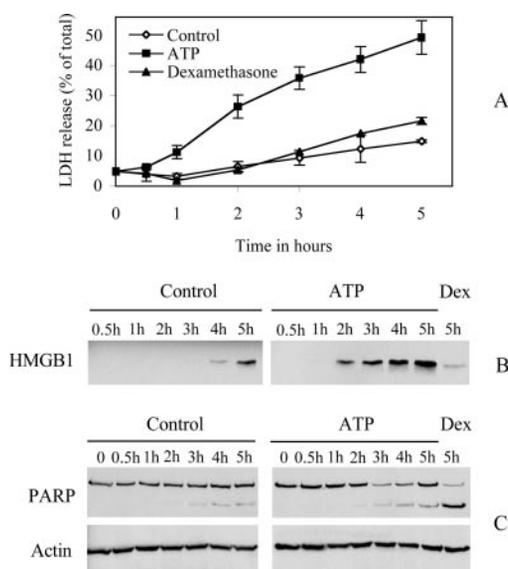
P2X7R Signaling Pathways in Thymocyte Death

FIG. 1. **P2X7R ligation leads to necrosis rather than apoptosis of thymocytes.** *A*, kinetics of LDH release from thymocytes treated with 1 mM ATP, 100 nM dexamethasone, or control buffer. The experiments were performed on 3 separate days, and the values represent the mean ± S.D. of three experiments. *B*, immunoblots performed with affinity-purified rabbit anti-HMGB1 antibody on culture supernatants of thymocytes incubated with 1 mM ATP or control buffer for increasing lengths of time, or with 100 nM dexamethasone (*Dex*) for 5 h. *C*, proteins from thymocyte lysates incubated with or without 1 mM ATP for increasing lengths of time or 100 nM dexamethasone (*Dex*) for 5 h were separated on 7.5% SDS-PAGE and immunoblotted with anti-PARP antibody (*C*, *top panels*). The same blots were stripped and probed for actin to show equal loading (*C*, *bottom panels*). The results shown in *B* and *C* are representative of at least two experiments performed on different days.

HMGB1 release during the same time. Cleavage of PARP is detected between 4 and 5 h following ATP treatment, and though to a greater extent than the untreated control, is much diminished compared with dexamethasone-treated thymocytes (Fig. 1*C*). These results indicate that the effector phase of thymocyte lysis is well underway 2 h after ATP treatment. The involvement of various death effector molecules and signaling pathways in subsequent experiments on thymocyte ATP-induced lysis was therefore determined at the 2-h time point.

Activation of the MAP Kinase^Erk1/2 Pathway Is Required for ATP-induced Thymocyte Death—The role of the various MAP kinase pathways in thymocyte lysis elicited by ATP was defined using specific inhibitors of the Erk1/2, p38 or JNK modules. Strong inhibition of LDH release was only observed after pre-treatment of thymocytes with 20 μM U0126, a MEK1/2 pharmacologic inhibitor. At the same dose, U0124, a negative control for U0126; SB 203580, an inhibitor of p38 kinase; and SP 600125, an inhibitor of JNK kinases, did not modulate cell death (Fig. 2*A*). ATP stimulation of thymocytes led to phosphorylation of Erk1/2, and the MEK inhibitor efficiently prevented this activation (Fig. 2*C*). Phosphorylation of Erk1/2 peaked at 15 min after ATP addition, then decreased rapidly at 30 min (Fig. 2*B*). The p38 and JNK1/2 kinases were also activated, and their phosphorylation increased over time (Fig. 2*B*). Although unable to inhibit LDH release from thymocytes treated with ATP, the specific inhibitors of the p38 and JNK pathways blocked anisomycin-induced phosphorylation of the two kinases (data not shown). Stimulation of thymocytes by ATP thus leads to cell death requiring activation of only the Erk1/2 pathway.

The protein phosphatases 1 and 2A are not involved in ATP-mediated thymocyte lysis, because pretreatment with okadaic acid, an inhibitor of both phosphatases, not only did not pre-
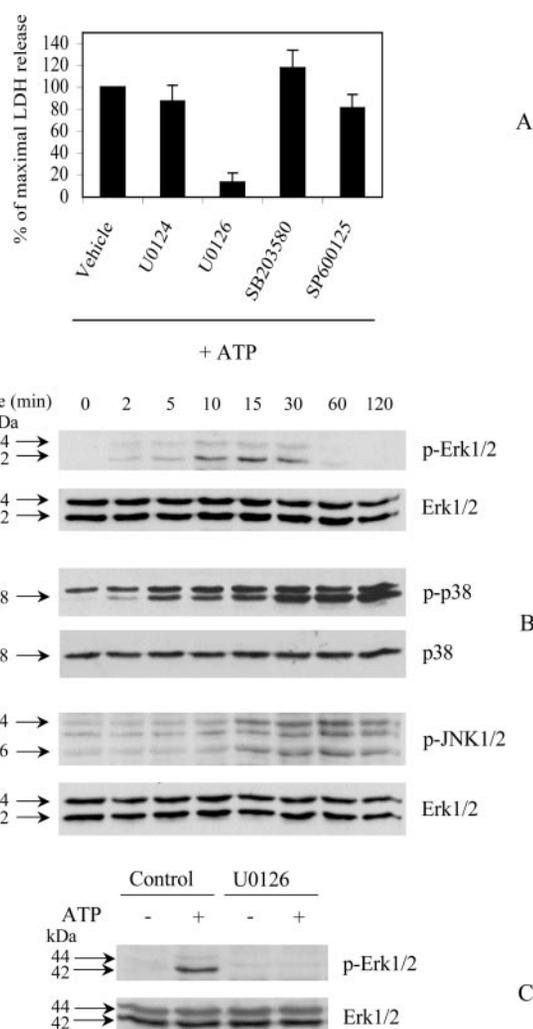

FIG. 2. **The MAP kinase Erk1/2 is involved in ATP induced cell death.** *A*, the effects of various inhibitors of MAP kinases or MAP kinase-kinase on ATP-induced LDH release. Thymocytes were preincubated for 1 h at 37 °C with 20 μM U0126, a specific inhibitor of MEK1/2; U0124, an inactive analog of U0126; SB 203580, an inhibitor of the p38 MAP kinase; SP600125, an inhibitor of the JNK MAP kinases; or with an equivalent volume of Me2SO (vehicle control). Thymocytes were then treated with 1 mM ATP for 2 h. The experiments were performed on 3 separate days, and the values represent the mean ± S.D. of three experiments. *B*, kinetic analysis of phosphorylation of the Erk1/2, JNK1/2, and p38 MAP kinases after P2X7R stimulation with 1 mM ATP. Thymocytes were treated with ATP for increasing lengths of time at 37 °C. Proteins from thymocyte lysates were separated on 10% SDS-PAGE and immunoblotted for phospho-threonine and phospho-tyrosine with anti-Erk1/2 (pTpY 185/187) (*B*, *first panel*) or anti-p38 (pTpY 180/182) (*B*, *third panel*) antibodies, or with anti-JNK1/2 (pTpY 183/185) antibody (*B*, *fifth panel*). After stripping, the three blots were probed with anti-total Erk1/2 (*B*, *second* and *last panels*) or anti-total p38 (*B*, *fourth panel*) antibodies to check for equal loading of gels. In *C*, thymocytes preincubated or not with U0126 were then treated with 1 mM ATP or control buffer for 15 min at 37 °C. Proteins from cell lysates were separated on 10% SDS-PAGE and immunoblotted for phospho-threonine and phospho-tyrosine with anti-Erk1/2 antibody (pTpY 185/187) (*C*, *top panel*). After stripping, the blot was probed for total anti-Erk1/2 (*C*, *bottom panel*). The results shown in *B* and *C* are typical of those obtained in three independent experiments.

vent cell death but instead increased it (Fig. 3*A*). It should be noted that, although okadaic acid alone increased significantly Erk1/2 phosphorylation (Fig. 3*B*), cell death remained at the level of control untreated thymocyte cultures (12% LDH release). ATP stimulation of okadaic acid-treated thymocytes potentiated Erk1/2 phosphorylation by 20%; this value was calculated with a shorter time of exposure by densitometry (data not shown). Using the inhibitor of MEK1/2 activities,
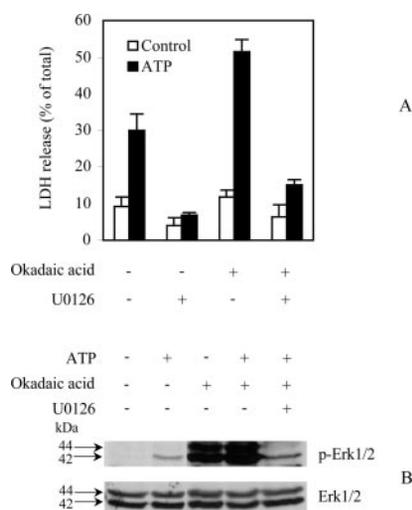
FIG. 3. **Inhibition of phosphatase activity by okadaic acid potentiates ATP induced cell death and MAP kinase[Erk1/2] phosphorylation.** *A*, thymocytes were preincubated with 1 μM okadaic acid or 20 μM U0126 or both inhibitors for 1 h at 37 °C. After stimulation with ATP for 2 h, the percentage of LDH release was determined. *B*, as above, thymocytes were preincubated with the same inhibitors for 1 h and stimulated with ATP for 15 min. Proteins from cellular lysates were separated on 10% SDS-PAGE and immunoblotted for phospho-threonine and phospho-tyrosine with anti-Erk1/2 (pTpY 185/187) antibody (*B, top panel*). After stripping, the blot was probed for total Erk1/2 antibody (*B, bottom panel*). The results are representative of three experiments performed on different days.

U0126, we found that ATP-induced LDH release was much diminished, whether or not okadaic acid was present (Fig. 3*A*). As expected, U0126 strongly inhibited the phosphorylation of Erk1/2, demonstrating that these MAP kinases are key mediators in ATP-induced cell death.

ATP-induced Erk1/2 Phosphorylation Is Mediated through the Purinergic Receptor P2X7—Mouse thymocytes express several P2X receptors, including P2X1R, -2R, -6R, and -7R (28). To identify which P2X receptor may be linked to Erk1/2 activation, we showed that pretreatment of thymocytes with the P2X7R antagonist, o-ATP, blocked the appearance of phosphorylated Erk1/2 following stimulation with ATP (Fig. 4*A*). Importantly, we found no activation of Erk1/2 in P2X7R-deficient thymocytes treated with ATP (Fig. 4*B*). This was not related to a P2X7R-dependent default in the Erk1/2 pathway itself, because phorbol 12-myristate 13-acetate could still activate Erk1/2 at identical levels in thymocytes from wild type or P2X7R-deficient mice (Fig. 4*C*). Furthermore, we determined by reverse transcription-PCR that, as in wild type animals, thymocytes from P2X7R-deficient mice express P2X1R, -2R, and -6R (data not shown). Taken together, these results indicate that Erk1/2 phosphorylation in murine thymocytes results from the ligation of P2X7R by ATP.

Role of Calcium in Thymocyte Death Elicited by ATP—The opening of ion channels leading to a rapid influx into the cytosol of divalent cations (in particular, Ca^{2+}) is characteristic of P2X7R activation (41). The role of Ca^{2+} in ATP-mediated P2X7R effects was therefore assessed. As shown in Fig. 5*A*, the level of ATP-induced LDH release was not affected by the absence of extracellular calcium, and Erk1/2 phosphorylation was identical in thymocytes whether or not calcium was present (Fig. 5*B*). Thus, stimulation of P2X7R by ATP leads to both thymocyte lysis and Erk1/2 phosphorylation in a calcium-independent way.

Src family Tyrosine Kinase(s) and PI3K Are Necessary for P2X7R-dependent Thymocyte Death—Because Src kinases are involved in T-cell receptor-dependent signal transduction in thymocytes (reviewed in Ref. 42), their involvement in the
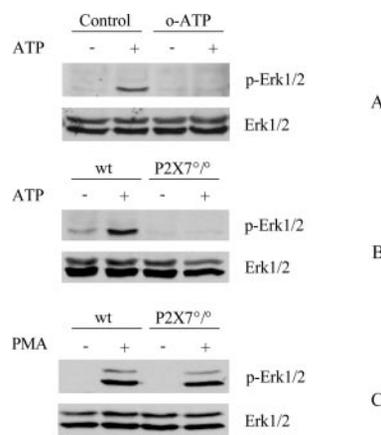

FIG. 4. **The MAP kinase[Erk1/2] is phosphorylated following P2X7R stimulation.** *A*, thymocytes were preincubated with 300 μM o-ATP or control buffer for 1 h at 37 °C and then stimulated with 1 mM ATP for 15 min. *B* and *C*, thymocytes from wild type (*wt*) or P2X7R-deficient (*P2X7°/°*) mice were incubated with 1 mM ATP or control buffer (*B*) or 1 μM phorbol 12-myristate 13-acetate (*PMA, C*). Proteins from cellular lysates were separated by SDS-PAGE and immunoblotted for phospho-threonine and phospho-tyrosine with anti-Erk1/2 (pTpY 185/187) antibody (*three top panels* of *A–C*). After stripping, the blots were probed for total Erk1/2 (*three bottom panels* of *A–C*). The results are representative of three experiments performed on different days.
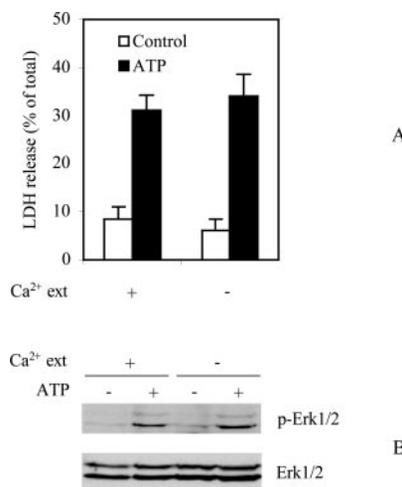

FIG. 5. **P2X7R-induced thymocyte death and phosphorylation of MAP kinase[Erk1/2] are calcium independent.** *A*, thymocytes were incubated in complete or Ca^{2+} free RPMI 1640 medium and stimulated or not with 1 mM ATP for 2 h at 37 °C. Percentage of LDH release was determined. The experiments were performed on 3 separate days, and the values represent the mean ± S.D. of three experiments. *B*, thymocytes treated as above were lysed, and proteins from cellular lysates were separated on 10% SDS-PAGE. The immunoblot was performed with rabbit anti-Erk1/2 (pTpY 185/187) antibody to detect phosphorylated Erk1/2, and re-probed for total Erk1/2 to show equal loading. The results are representative of three experiments performed on different days.

P2X7R signaling pathway was investigated. The effect of inhibitors of Src kinases on thymocyte death was evaluated, and the phosphorylation state of Src kinases in cell lysates was determined, using rabbit anti-Src (pY[418]) phosphospecific antibodies. Genistein, a broad spectrum tyrosine kinase inhibitor, and PP2, a selective inhibitor of the Src family tyrosine kinase(s), significantly diminished ATP-induced thymocyte lysis (Fig. 6*A*). Src phosphorylation increased in ATP-stimulated thymocyte lysates, and phosphorylation could be blocked by PP2, providing additional support for a role of Src family tyrosine kinase(s) in P2X7R-induced thymocyte death (Fig. 6*B*).

To identify the Src family tyrosine kinase(s) involved in P2X7R signaling, thymocyte lysates were precipitated with
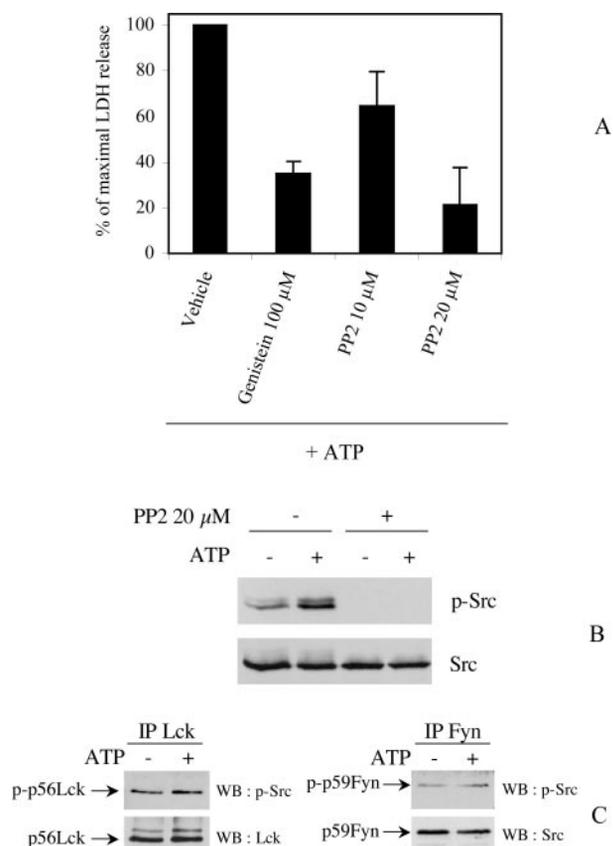
FIG. 6. **The Src family tyrosine kinase is phosphorylated after P2X7R stimulation and is involved in P2X7R-mediated thymocyte death.** *A*, thymocytes were preincubated with different tyrosine-kinase inhibitors or vehicle control for 1 h at 37 °C. Genistein was used at 100 μM and PP2 at two different concentrations (10 and 20 μM). After stimulation with 1 mM ATP for 2 h at 37 °C, percentages of ATP-induced LDH release were determined. The experiments were performed on 3 separate days, and the values represent the mean ± S.D. of three experiments. *B*, thymocytes were preincubated with 20 μM PP2 or control buffer and then stimulated with ATP for 5 min. Proteins from cellular lysates were separated on 10% SDS-PAGE and immunoblotted with phosphospecific anti-Src (pY418) antibody. After stripping, the blot was probed for total Src kinase. *C*, thymocytes were treated with ATP or control buffer for 5 min at 37 °C. Cells were lysed in a lysis buffer containing phosphatase inhibitors (see "Materials and Methods"). The kinases, Lck or Fyn, were specifically immunoprecipitated with anti-Lck or anti-Fyn mouse mAbs, respectively (*C*, Lck, *left panel*; and Fyn, *right panel*). Immunoprecipitated kinases were analyzed on 10% SDS-PAGE and immunoblotted with phosphospecific anti-Src (pY418) antibody. After stripping, the blots were probed for total Lck with an anti-Lck mouse mAb and for total Fyn with anti-Src antibody. The results shown in *B* and *C* are representative of at least two experiments performed on different days. *IP*, immunoprecipitation; *WB*, Western blot.

mAb specific for p56^{lck} and p59^{fyn}, and the immunoprecipitates were subsequently analyzed with rabbit anti-Src phosphospecific antibodies. Significantly, the two Src-tyrosine kinases p56^{lck} and p59^{fyn} are known to be recruited during T cell receptor-mediated signal transduction in thymocytes (reviewed in Ref. 42). However, no phosphorylation of either kinase was revealed in lysates of ATP-stimulated thymocytes (Fig. 6*C*). It thus appears that neither p56^{lck} nor p59^{fyn} play a role in the transduction pathway activated by ligation of the P2X7R by ATP.

PI4K has been identified by proteomic analysis to be 1 of 11 proteins associated with the purinergic receptor P2X7 (43). To determine whether PI4K or related kinases participate in the P2X7R signaling pathway, we treated thymocytes with wortmannin, an inhibitor of PI4K and PI3K, or with LY294002, a selective inhibitor of PI3K, and measured ATP-triggered LDH release. A significant decrease in thymocyte lysis was observed
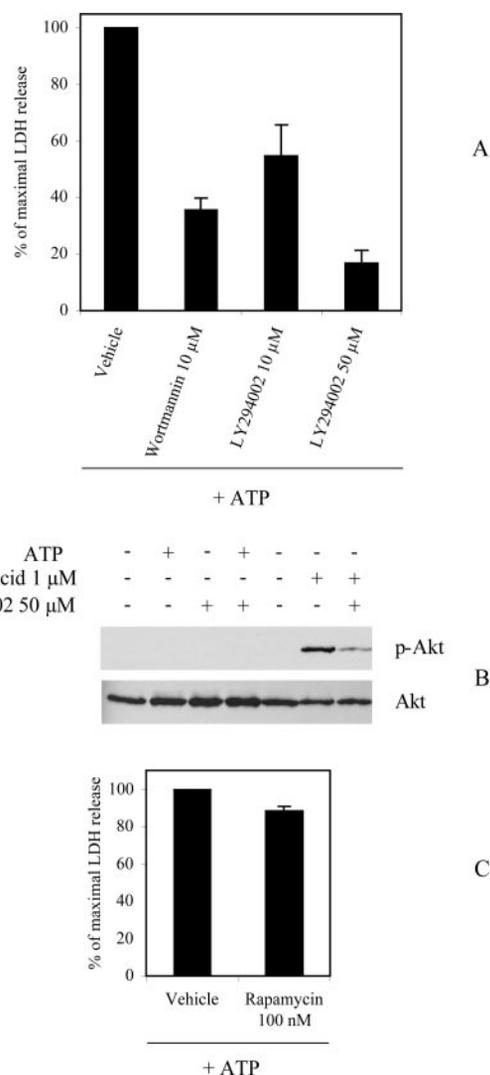

FIG. 7. **PI3K is involved in P2X7R-mediated thymocyte death.** *A*, thymocytes were preincubated with different PI3K inhibitors (wortmannin or LY294002) or the same volume of vehicle control for 1 h at 37 °C. Percentages of LDH release were measured 2 h after ATP addition. *B*, thymocytes were preincubated with 1 μM okadaic acid or 50 μM LY294002 or both for 1 h at 37 °C. Cells were stimulated with 1 mM ATP or control buffer for 15 min. Proteins from thymocyte lysates were separated on 10% SDS-PAGE and immunoblotted with anti-phospho Akt (pS473) antibody (*B*, *top panel*). The membrane was stripped and probed for total Akt with anti-Akt1 (*B*, *bottom panel*). The results are representative of three experiments performed on different days. *C*, thymocytes were pretreated with 100 nM rapamycin or with the same volume of vehicle control for 1 h at 37 °C. Percentages of LDH release were determined after stimulation with 1 mM ATP for 2 h. The experiments were performed on 3 separate days, and the values represent the mean ± S.D. of three experiments.

for both inhibitors (Fig. 7*A*). The phosphorylation status of Akt, one of the target enzymes downstream of PI3K, was then examined. As shown in Fig. 7*B*, ATP did not activate Akt, unlike okadaic acid, and the phosphorylation induced by okadaic acid was inhibited by the selective inhibitor of PI3K. The lack of effect on thymocyte lysis of rapamycin, a highly specific inhibitor of mammalian target of rapamycin, a substrate of Akt, confirms the inability of ATP to trigger the phosphorylation and activation of Akt (Fig. 7*C*). These results show that, although PI3K is involved in the P2X7R biochemical death pathway, the effective downstream protein kinases do not include Akt.

Role for the Proteasome in ATP-mediated Thymocyte Death—Because some forms of cell death rely on the proteasome and
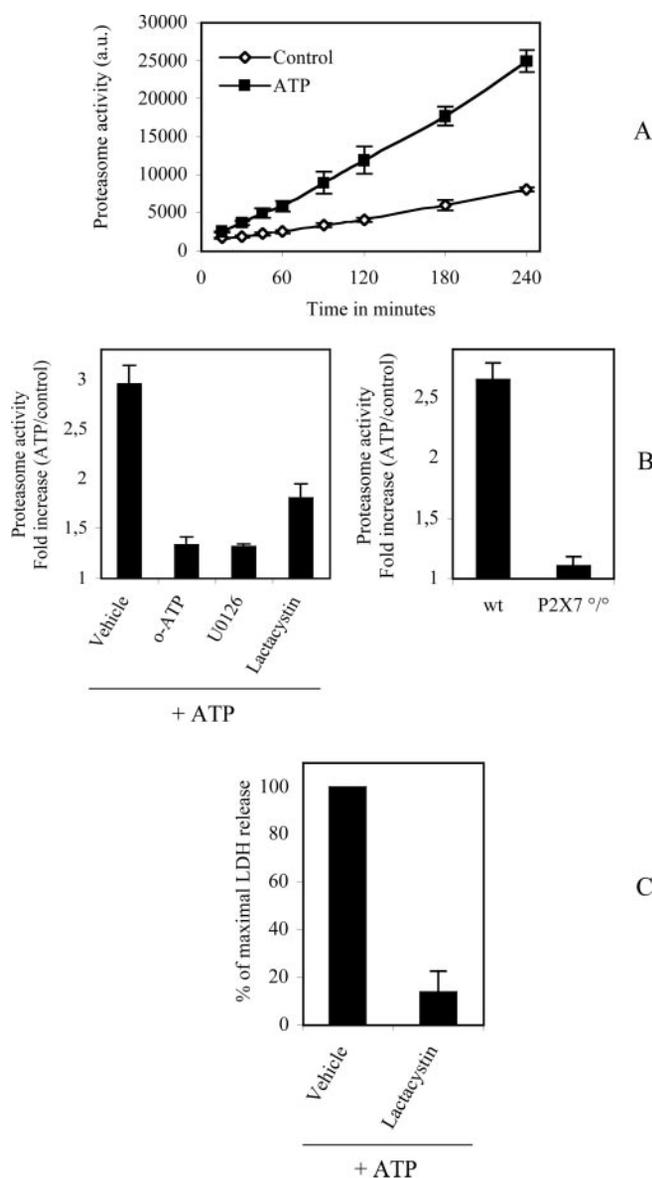
FIG. 8. **The proteasome plays a role in P2X7R-triggered thymocyte death.** *A*, thymocytes were stimulated with 1 mM ATP or vehicle control for 2 h and incubated with 20 μM of the fluorogenic peptide substrate, Suc-Leu-Leu-Val-Tyr-AMC, for an additional 2 h at 37 °C. The increase in fluorescence over time was determined with a spectrofluorometer, as described under "Materials and Methods." *B* (*left inset*), thymocytes from BALB/c mice were incubated with optimal concentrations of o-ATP (300 μM), U0126 (20 μM), or lactacystin (10 μM) for 1 h at 37 °C. After incubation, cells were treated with ATP or control buffer for 2 h, and the fluorogenic substrate was added for an additional 2 h. The -fold increases in fluorescence after ATP treatment, compared with unstimulated cells, were determined by measuring the fluorescence in each sample. *B* (*right inset*), thymocytes from wild type (*wt*) and P2X7R-deficient (*P2X7°/°*) animals were treated as above. The -fold increases in fluorescence after ATP stimulation, compared with resting cells, were determined. *C*, thymocytes were incubated with 10 μM lactacystin or control buffer for 1 h at 37 °C, and then stimulated with 1 mM ATP for 2 h. Percentages of LDH release were determined. The experiments were performed on 3 separate days, and the values represent the mean ± S.D. of three experiments.

FIG. 9. **Different enzymes are involved sequentially in the P2X7R-mediated thymocyte death pathway.** Thymocytes were treated with control buffer or the inhibitors, PP2 (20 μM), LY294002 (50 μM), U0126 (20 μM), or lactacystin (10 μM) for 1 h at 37 °C. After incubation, they were stimulated with 1 mM ATP for 5 min. Proteins from cellular lysates were separated on 10% SDS-PAGE and immunoblotted with phosphospecific anti-Src (pY418) antibody (*A, upper blot*) or for phospho-threonine and phospho-tyrosine with anti-Erk1/2 (pTpY 185/187) antibodies (*B, upper blot*). After stripping, the blots were probed for total Src kinase (*A, lower blot*) or total Erk1/2 (*B, lower blot*). The results shown are representative of three experiments performed on different days.

NF-κB pathway (44–47), we examined proteasome function in ATP-treated thymocytes to determine whether the proteasome could be involved in thymocyte death downstream of PI3K. Chymotrypsin-like proteasome activity was measured using a fluorogenic peptide substrate and found to increase 3-fold in ATP-treated thymocytes, compared with control cells (Fig. 8*A*). P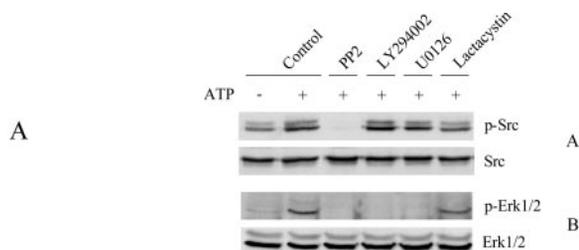roteasome activation was dependent on P2X7R stimulation, because it was not observed in thymocytes pretreated with o-ATP or derived from P2X7R-deficient mice (Fig. 8*B*). Pretreatment with lactacystin, a highly specific proteasome inhibitor, prevented lysis of ATP-treated thymocytes (Fig. 8*C*). These findings imply an involvement for the proteasome in the P2X7R signal transduction pathway.

Hierarchy of Activation of Mediators in the P2X7R-dependent Pathway Leading to Cell Death—The order in which enzymes involved in the P2X7R signaling cascade are activated was established by determining the effect of various pharmacological inhibitors on the phosphorylation status of different kinases. P2X7R stimulation with ATP for 5 min led to an increase in the phosphorylation of Src family kinases. Significantly, this phosphorylation was inhibited by PP2 but not LY294002, U0126, or lactacystin (Fig. 9*A*). These results suggest that Src kinases are independent or upstream of PI3K, MEK1/2, and the proteasome. PP2, LY294002, and U0126 blocked the phosphorylation of Erk1/2, whereas lactacystin had no effect (Fig. 9*B*). The MAP kinase module is thus downstream of Src kinase and PI3K, but it is independent or upstream of the proteasome. Both lactacystin and U0126 inhibit the P2X7R-stimulated proteolytic activity of the proteasome (Fig. 8*B*), indicating that activation of the proteasome is regulated by the MAP kinase$^{Erk1/2}$ module and is downstream of MEK1/2.

Non-selective Pore Formation Is Not Modulated by the Mediators of the P2X7R Signaling Pathway—Activation of P2X7R by extracellular ATP rapidly induces the opening of a non-selective pore. The effect of different inhibitors of the P2X7R signaling cascade on pore opening was therefore tested. Mouse thymocytes were incubated with or without the inhibitors and stimulated or not with 1 mM ATP for 15 min in the presence of the immunofluorescent YO-PRO-1 iodide and propidium iodide. They were then washed and kept at 4 °C until analyzed by flow cytometry. As shown in Fig. 10*A*, ATP induced the uptake of YO-PRO-1 in about 45% of the thymocytes. This was related to ATP ligation of P2X7R, because preincubation with o-ATP reduced the number of YO-PRO-1-positive thymocytes to 8%. The inhibitors of MEK1/2, Src family kinase(s), PI3K, and proteasome, had no effect on P2X7R-mediated YO-PRO-1 uptake (Fig. 10*B*), indicating that pore formation is independent of the ATP-induced intracellular signaling events leading to thymocyte lysis.

However, this finding does not exclude the possibility that the non-selective pore may influence activation of the enzymes involved in the cell death pathway. To address this question, we took advantage of the Pro-451 to Leu mutation of P2X7R in C57BL/6 mice, which is responsible for a reduction in ATP-
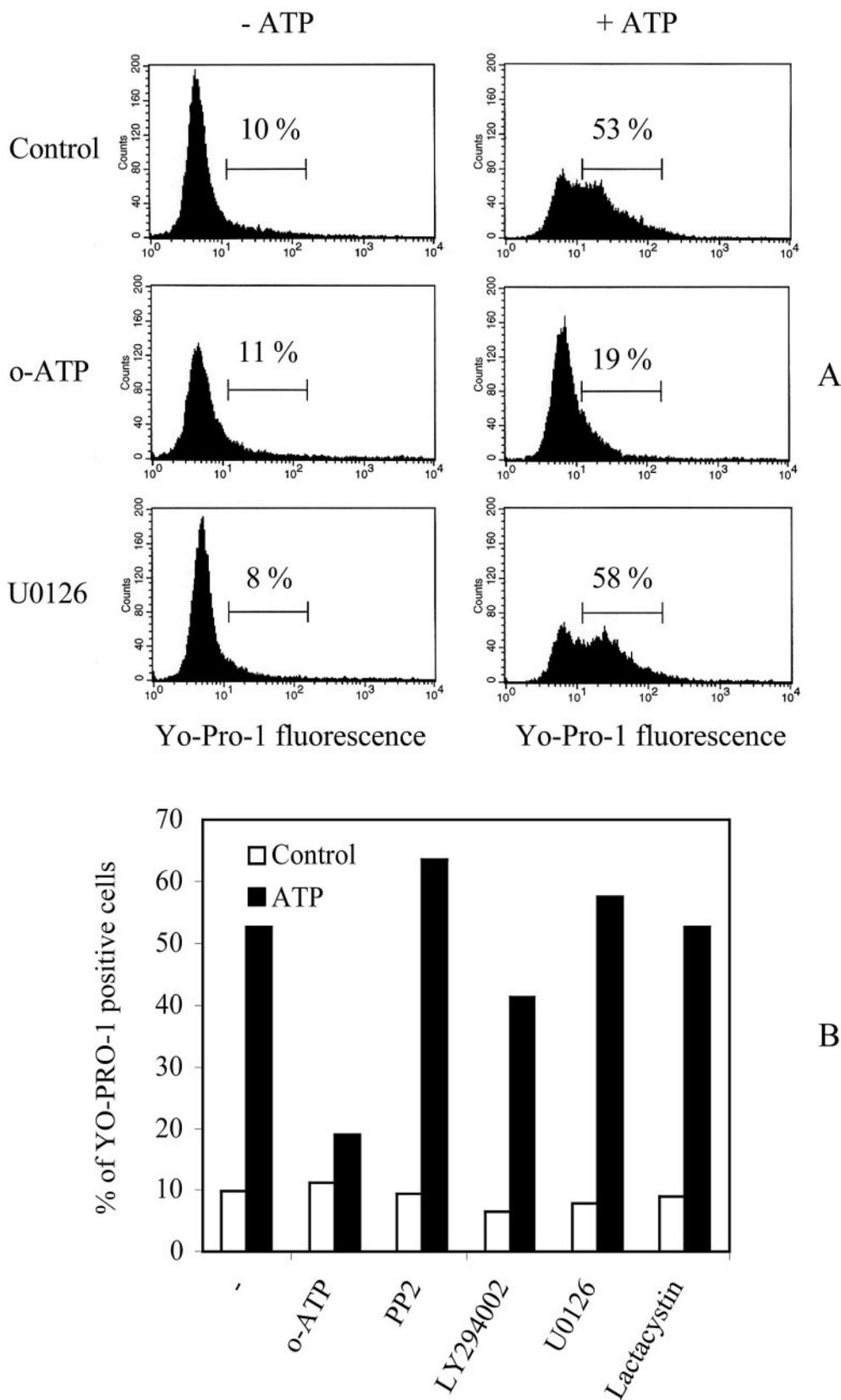
FIG. 10. **The formation of the non-selective pore is upstream and/or independent of the enzymatic cascade triggered by P2X7R.** *A*, thymocytes were treated with control buffer or optimal concentrations of o-ATP (300 μM) or U0126 (20 μM) for 1 h at 37 °C. Cells were then incubated with 2 μM YO-PRO-1 and stimulated with 1 mM ATP (+*ATP*) or control buffer (−*ATP*) for 15 min. Cells were centrifuged and kept on ice at 4 °C in an assay buffer containing propidium iodide. Propidium iodide-positive cells were excluded, and YO-PRO-1-positive cells were quantified by flow cytometry. The results shown are representative of three experiments performed on different days. *B*, percentages of YO-PRO-1-positive cells are presented as histograms. Thymocytes were treated with control buffer or o-ATP, PP2, LY294002, U0126, or lactacystin at optimal concentrations for 1 h at 37 °C. Cells were then incubated with 2 μM YO-PRO-1 and stimulated with 1 mM ATP (+*ATP*) or control buffer (−*ATP*) for 15 min. Cells were centrifuged and kept on ice at 4 °C in an assay buffer containing propidium iodide. Propidium iodide-positive cells were excluded, and YO-PRO-1-positive cells were quantified by flow cytometry. The experiments were performed on 3 separate days, and the values represent the mean ± S.D. of three experiments.
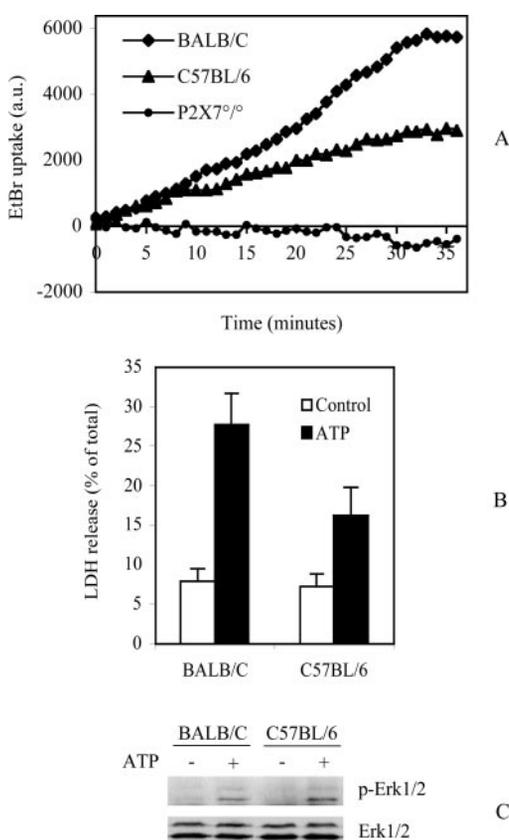
FIG. 11. **The level of thymocyte death correlates with non-selective pore formation.** *A*, thymocytes from BALB/c, C57BL/6, and P2X7R-deficient mice were incubated with EtBr and stimulated with 1 mM ATP for increasing lengths of time. EtBr fluorescence of each sample was monitored for 35 min at 37 °C. For each curve, ATP-dependent EtBr uptake was calculated by subtracting EtBr values of unstimulated cells from values of ATP-stimulated thymocytes. *B*, thymocytes from BALB/c and C57BL/6 mice were stimulated or not with 1 mM ATP for 2 h at 37 °C. Percentages of LDH release were determined. The experiments were performed on 3 separate days, and the values represent the mean ± S.D. of three experiments. *C*, thymocytes from BALB/c and C57BL/6 mice were stimulated with ATP for 15 min at 37 °C. Proteins from cellular lysates were separated on 10% SDS-PAGE and immunoblotted for phospho-threonine and phospho-tyrosine with anti-Erk1/2 (pTpY 185/187) antibody (*C*, *top blot*). After stripping, the blots were probed for total Erk1/2 (*C*, *lower blot*). The results shown in *A* and *C* are representative of three experiments performed on different days.

mediated pore formation (4). Pore formation, as assessed by EtBr uptake after stimulation with various concentrations of ATP, was compared in thymocytes derived from C57BL/6 and BALB/c mice. For both strains, the optimal concentration for pore formation was 1 mM ATP (data not shown), at which concentration BALB/c thymocytes incorporated twice as much EtBr as cells from C57BL/6 mice, whereas no EtBr uptake was detected in P2X7R-deficient cells (Fig. 11*A*). Likewise, LDH release from ATP-stimulated BALB/c thymocytes was twice that observed for C57BL/6 mice (Fig. 11*B*). However, we found no differences in P2X7R mRNA levels nor P2X7R expression between thymocytes from BALB/c and C57BL/6 mice (Fig. 12). Importantly, Erk1/2 phosphorylation was identical when thymocytes from BALB/c and C57BL/6 mice were compared (Fig. 11*C*), implying that the non-selective pore does not affect Erk1/2 activation.

DISCUSSION

The present work was focused on the intracellular signaling events activated by the ligation of P2X7R by ATP and leading to cell death in murine thymocytes. Under our experimental
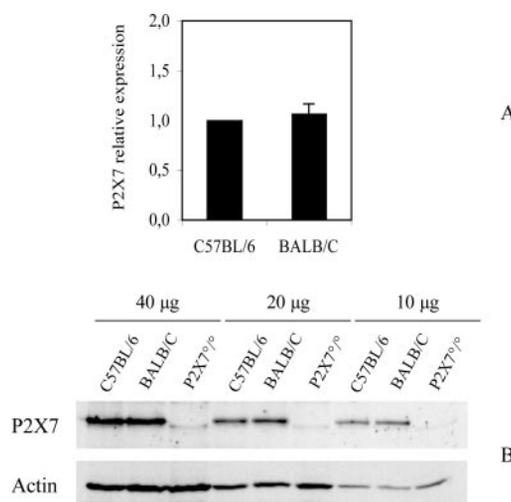

FIG. 12. **P2X7R mRNA and protein expression is identical in thymocytes from C57BL/6 and BALB/c mice.** *A*, thymocytes from C57BL/6 and BALB/c mice were isolated, and RNA was extracted as described under "Materials and Methods." 2 μg of total RNA was reverse-transcribed, and P2X7R expression was determined using real-time PCR and normalized to that of actin. *B*, 1×10^7 thymocytes from C57BL/6, BALB/c, and P2X7R-deficient mice were lysed and 40, 20, and 10 μg of proteins were separated by SDS-PAGE and transferred to nitrocellulose membrane. Blots were immunostained with affinity-purified rabbit anti-P2X7R or goat anti-actin antibodies.

conditions, the main pathway of P2X7R-mediated thymocyte death was necrosis/lysis, rather than apoptosis. The biochemical events underlying P2X7R signaling were identified following a 2-h stimulation of thymocytes with ATP. At this time point, there was significant release of HMGB1 in ATP-treated thymocytes, compared with untreated or dexamethasone-treated thymocytes. HMGB1 is released only by necrotic cells, whereas in apoptotic cells, even at later stages of cell death, this nuclear protein is tightly bound to deacetylated histone (40). Concomitantly, cleavage of PARP, a substrate of caspase-3, was barely detectable and, compared with dexamethasone-exposed thymocytes, was much reduced even after a 5-h treatment with ATP. The prevalence of necrosis in P2X7R-induced thymocyte death agrees with the report of Le Stunff *et al.* (31), who found only a slight increase over controls of ATP-induced terminal deoxynucleotidyl transferase-mediated dUTP nick end labeling-positive thymocytes.

Stimulation of murine thymocytes with ATP induced the activation of Erk1/2, p38, and JNK1/2 MAP kinase modules. However, a role in thymocyte death was established for only Erk1/2, because LDH release was inhibited by U0126, a specific pharmacological inhibitor of MEK1/2, but not by p38 or JNK inhibitors. Phosphorylation of Erk1/2 correlated with thymocyte death and was dependent on ATP-stimulated P2X7R. It was much reduced in thymocytes pre-treated with o-ATP, a P2X7R antagonist, and was not observed in ATP-treated P2X7R-deficient thymocytes.

The involvement of Erk1/2 in thymocyte death is intriguing, because MAP kinase Erk1/2 activation is very often linked with cell proliferation and differentiation (48). However, Erk1/2 phosphorylation is needed for neuronal cell death induced by glutamate (49) or genistein (50). Paraptosis mediated by insulin-like growth factor I receptor requires the activation of Erk1/2 and JNK pathways (51). In addition, during positive selection in the thymus, production of phosphorylated Erk1/2 is slow and prolonged, whereas it is potent and short-lived in thymocytes undergoing negative selection (52, 53).

The activation of the MAP kinase pathways following P2X7R stimulation is not restricted to murine thymocytes. Phospho-

rylation of Erk1/2 associated or not with activation of p38 or JNK MAP kinases has been reported for cells of different lineages (32, 34, 54–57). It is noteworthy that P2X7R stimulation of the cell lines used in the previous reports did not always lead to cell death, and no correlation between MAP kinase activation and cell death could be deduced. In ATP-treated thymocytes, the phosphorylation of p38 and JNK MAP kinases is not linked to cell death, because inhibition of either had no effect on LDH release. Similarly, P2X7R-mediated JNK activation in BAC1 macrophages plays no role in apoptosis (58).

ATP stimulation of P2X7R leads to formation of plasma membrane cationic channels, allowing the influx of extracellular Ca^{2+}. P2X7R-induced thymocyte lysis and Erk1/2 phosphorylation are independent of extracellular calcium. Moreover, chelation of intracellular calcium with 1,2-bis(2-aminophenoxy)ethane-N,N,N',N'-tetraacetic acid tetrakis not only did not prevent death but instead increased it (data not shown). Erk1/2 phosphorylation is also Ca^{2+}-independent in rat P2X7R-transfected HEK 293 cells (55) and parotid acinar cells (59). Calcium influx is, on the other hand, needed for Erk1/2 activation in astrocytoma (32) and Jurkat cells (54). Using various deletion mutants of rat P2X7R, Amstrup *et al.* (55) have concluded that the N-terminal domain of P2X7R is essential for triggering Erk1/2 phosphorylation, whereas the C terminus domain controls Ca^{2+} entry, suggesting that the two events may be dissociable in many cell types.

Our data clearly establish a role, upstream of the MAP kinase[Erk1/2] module, for Src kinases in P2X7R-induced thymocyte necrosis, because both Erk1/2 phosphorylation and cell death were abolished by an inhibitor of Src family tyrosine kinase(s). However, neither p56[*lck*] nor p59[*fyn*] represent the relevant kinase. The involvement of Src family tyrosine kinase(s) in P2X7R signaling has been described for rat microglia (60) and for Jurkat lymphoma (54) and astrocytoma cells (32).

A proteomic study has identified eleven proteins that interact with P2X7R, including the lipid kinase phosphatidylinositol 4-kinase, suggesting that lipid production may be involved in P2X7R signaling pathways (43). Our results are consistent with PI4K and PI3K being P2X7R signaling mediators, because a broad spectrum inhibitor of phosphatidylinositol kinases and a specific PI3K inhibitor reduced ATP-induced LDH release. Unexpectedly, PI3K activation did not lead to Akt activation, because no phosphorylated Akt was detected in ATP-treated thymocytes, and inhibition by rapamycin of the Akt substrate mammalian target of rapamycin had no effect on ATP-mediated thymocyte death. Pretreatment of thymocytes with the PI3K inhibitor prevented the phosphorylation of Erk1/2 but not of the Src family tyrosine kinase(s), indicating that P2X7R signaling in thymocytes leads to Erk1/2 phosphorylation via sequential activation of Src family tyrosine kinase(s), PI3K and MEK1/2. Alternatively, P2X7R stimulation may activate two independent pathways, involving Src family tyrosine kinase(s) and PI3K, both leading to MEK1/2 activation. Jacques-Silva *et al.* (61) have recently shown the activation of Akt via PI3K and Src family kinases in P2X7R-stimulated rat astrocytes. This observation contrasts with our finding that Akt is not phosphorylated in ATP-treated thymocytes, despite PI3K activation. Akt is usually associated with cell survival (reviewed in Ref. 62), which is compatible with the resistance of astrocytes to P2X7R-mediated cell death (63).

The measurement of proteasome activity in ATP-treated thymocytes suggested a role for the proteasome in the P2X7R transduction pathway. Moreover, a proteasome inhibitor blocked LDH release but had no effect on the phosphorylation of Src family tyrosine kinase(s) and Erk1/2, suggesting that proteasomal proteolysis occurs downstream of these signaling

events. In addition, a MEK1/2 inhibitor decreased the ATP-mediated chymotrypsin-like activity of the 20 S proteasome, confirming that the Erk1/2 MAP kinase module is located upstream of the proteasome. Proteasome activation has also been observed in thymocyte apoptosis induced by ionizing radiation, glucocorticoids, or T cell receptor cross-linking (44–47). In mouse microglial cell line(s), proteasome activity is required for ATP-triggered P2X7R NF-κB activation and target gene expression (36) but not for apoptotic cell death (20). However, we found that P2X7R-mediated thymocyte death requires neither transcription nor translation, suggesting that NF-κB may be activated but does not affect thymocyte death.

In addition to being a ligand-gated ion channel, P2X7R has the ability to form a non-selective pore after repeated or prolonged ATP stimulation (64). In ATP-treated thymocytes, none of the P2X7R signaling mediators which we have identified modulated the formation of the non-selective pore, indicating that pore formation is independent and/or takes place upstream of the signaling cascade leading to cell death. At variance with our results, a role for second messengers in P2X7R pore opening, in particular, calcium, p38 MAP kinase, and MEK, has recently been reported for other cellular models (56, 57).

To address the issue of a link between P2X7R-mediated thymocyte death and pore formation, we compared these events in BALB/c and C57BL/6 thymocytes. Although the P2X7R of C57BL/6 bears a Pro-451 to Leu mutation that impairs non-selective pore formation (4), we found no differences between the two mouse strains in terms of P2X7R mRNA and protein expression. We have interpreted the large increase in pore formation and thymocyte lysis observed in BALB/c, compared with C57BL/6 thymocytes, as indicating that thymocyte death correlates with non-selective pore formation. Interestingly, phosphorylation of Erk1/2 was identical in ATP-treated thymocytes from both mouse strains, providing additional support for non-selective pore formation being unrelated to MAP kinase[Erk1/2] activation.

P2X7R-triggered reversible phosphatidylserine exposure on thymocytes also occurs independently of Erk1/2 activation, because it was not abolished by inhibitors of the Src family tyrosine kinase(s) or MEK1/2 (data not shown).

In summary, the C-terminal region of P2X7R regulates phosphatidylserine exposure (4) and non-selective pore formation (3–5). These two events are independent of the signaling pathway leading to Erk1/2 activation, whose control may depend on the N-terminal region of P2X7R (55). To the best of our knowledge, this is the first report implicating a role for both activation of MAP kinase[Erk1/2] and non-selective pore opening in P2X7R-mediated thymocyte death.

REFERENCES

1. Ralevic, V., and Burnstock, G. (1998) *Pharmacol. Rev.* **50,** 413–492
2. Torres, G. E., Egan, T. M., and Voigt, M. M. (1999) *J. Biol. Chem.* **274,** 6653–6659
3. Gu, B. J., Zhang, W., Worthington, R. A., Sluyter, R., Dao-Ung, P., Petrou, S., Barden, J. A., and Wiley, J. S. (2001) *J. Biol. Chem.* **276,** 11135–11142
4. Adriouch, S., Dox, C., Welge, V., Seman, M., Koch-Nolte, F., and Haag, F. (2002) *J. Immunol.* **169,** 4108–4112
5. Smart, M. L., Gu, B., Panchal, R. G., Wiley, J., Cromer, B., Williams, D. A., and Petrou, S. (2003) *J. Biol. Chem.* **278,** 8853–8860
6. North, R. A. (2002) *Physiol. Rev.* **82,** 1013–1067
7. Chiozzi, P., Sanz, J. M., Ferrari, D., Falzoni, S., Aleotti, A., Buell, G. N., Collo, G., and Di Virgilio, F. (1997) *J. Cell Biol.* **138,** 697–706
8. Falzoni, S., Chiozzi, P., Ferrari, D., Buell, G., and Di Virgilio, F. (2000) *Mol. Biol. Cell* **11,** 3169–3176
9. Colomar, A., Marty, V., Medina, C., Combe, C., Parnet, P., and Amedee, T. (2003) *J. Biol. Chem.* **278,** 30732–30740

10. Kahlenberg, J. M., and Dubyak, G. R. (2004) *Am. J. Physiol.* **286,** C1100–C1108
11. Solle, M., Labasi, J., Perregaux, D. G., Stam, E., Petrushova, N., Koller, B. H., Griffiths, R. J., and Gabel, C. A. (2001) *J. Biol. Chem.* **276,** 125–132
12. MacKenzie, A., Wilson, H. L., Kiss-Toth, E., Dower, S. K., North, R. A., and Surprenant, A. (2001) *Immunity* **15,** 825–835
13. Gu, B., Bendall, L. J., and Wiley, J. S. (1998) *Blood* **92,** 946–951
14. Gu, B. J., Zhang, W. Y., Bendall, L. J., Chessell, I. P., Buell, G. N., and Wiley, J. S. (2000) *Am. J. Physiol.* **279,** C1189–C1197
15. Lammas, D. A., Stober, C., Harvey, C. J., Kendrick, N., Panchalingam, S., and Kumararatne, D. S. (1997) *Immunity* **7,** 433–444
16. Kusner, D. J., and Adams, J. (2000) *J. Immunol.* **164,** 379–388
17. Coutinho-Silva, R., Stahl, L., Raymond, M. N., Jungas, T., Verbeke, P., Burnstock, G., Darville, T., and Ojcius, D. M. (2003) *Immunity* **19,** 403–412
18. Virginio, C., MacKenzie, A., North, R. A., and Surprenant, A. (1999) *J. Physiol.* **519,** 335–346
19. Wilson, H. L., Wilson, S. A., Surprenant, A., and North, R. A. (2002) *J. Biol. Chem.* **277,** 34017–34023
20. Ferrari, D., Los, M., Bauer, M. K., Vandenabeele, P., Wesselborg, S., and Schulze-Osthoff, K. (1999) *FEBS Lett.* **447,** 71–75
21. Zheng, L. M., Zychlinsky, A., Liu, C. C., Ojcius, D. M., and Young, J. D. (1991) *J. Cell Biol.* **112,** 279–288
22. Apasov, S. G., Koshiba, M., Chused, T. M., and Sitkovsky, M. V. (1997) *J. Immunol.* **158,** 5095–5105
23. Chiozzi, P., Murgia, M., Falzoni, S., Ferrari, D., and Di Virgilio, F. (1996) *Biochem. Biophys. Res. Commun.* **218,** 176–181
24. Le Feuvre, R. A., Brough, D., Iwakura, Y., Takeda, K., and Rothwell, N. J. (2002) *J. Biol. Chem.* **277,** 3210–3218
25. Coutinho-Silva, R., Persechini, P. M., Bisaggio, R. D., Perfettini, J. L., Neto, A. C., Kanellopoulos, J. M., Motta-Ly, I., Dautry-Varsat, A., and Ojcius, D. M. (1999) *Am. J. Physiol.* **276,** C1139–C1147
26. Ferrari, D., La Sala, A., Chiozzi, P., Morelli, A., Falzoni, S., Girolomoni, G., Idzko, M., Dichmann, S., Norgauer, J., and Di Virgilio, F. (2000) *FASEB J.* **14,** 2466–2476
27. Chvatchko, Y., Valera, S., Aubry, J. P., Renno, T., Buell, G., and Bonnefoy, J. Y. (1996) *Immunity* **5,** 275–283
28. Freedman, B. D., Liu, Q. H., Gaulton, G., Kotlikoff, M. I., Hescheler, J., and Fleischmann, B. K. (1999) *Eur. J. Immunol.* **29,** 1635–1646
29. Koshiba, M., Apasov, S., Sverdlov, V., Chen, P., Erb, L., Turner, J. T., Weisman, G. A., and Sitkovsky, M. V. (1997) *Proc. Natl. Acad. Sci. U. S. A.* **94,** 831–836
30. el-Moatassim, C., and Dubyak, G. R. (1992) *J. Biol. Chem.* **267,** 23664–23673
31. Le Stunff, H., Auger, R., Kanellopoulos, J., and Raymond, M. N. (2004) *J. Biol. Chem.* **279,** 16918–16926
32. Gendron, F. P., Neary, J. T., Theiss, P. M., Sun, G. Y., Gonzalez, F. A., and Weisman, G. A. (2003) *Am. J. Physiol.* **284,** C571–C581
33. Verhoef, P. A., Estacion, M., Schilling, W., and Dubyak, G. R. (2003) *J. Immunol.* **170,** 5728–5738
34. Pfeiffer, Z. A., Aga, M., Prabhu, U., Watters, J. J., Hall, D. J., and Bertics, P. J. (2004) *J. Leukoc. Biol.* **75,** 1173–1182
35. Parvathenani, L. K., Tertyshnikova, S., Greco, C. R., Roberts, S. B., Robertson, B., and Posmantur, R. (2003) *J. Biol. Chem.* **278,** 13309–13317
36. Ferrari, D., Wesselborg, S., Bauer, M. K., and Schulze-Osthoff, K. (1997) *J. Cell Biol.* **139,** 1635–1643
37. Ferrari, D., Stroh, C., and Schulze-Osthoff, K. (1999) *J. Biol. Chem.* **274,** 13205–13210
38. Etore, F., Tenu, J. P., Teiger, E., Adnot, S., Lonchampt, M. O., Pirotzki, E., and Le Doan, T. (1998) *Biochem. Pharmacol.* **55,** 1465–1473
39. Michel, A. D., Chessell, I. P., and Humphrey, P. P. (1999) *Naunyn-Schmiedeberg's Arch. Pharmacol.* **359,** 102–109
40. Scaffidi, P., Misteli, T., and Bianchi, M. E. (2002) *Nature* **418,** 191–195
41. Bianchi, B. R., Lynch, K. J., Touma, E., Niforatos, W., Burgard, E. C., Alexander, K. M., Park, H. S., Yu, H., Metzger, R., Kowaluk, E., Jarvis, M. F., and van Biesen, T. (1999) *Eur. J. Pharmacol.* **376,** 127–138
42. Anderson, S. J., Levin, S. D., and Perlmutter, R. M. (1994) *Adv. Immunol.* **56,** 151–178
43. Kim, M., Jiang, L. H., Wilson, H. L., North, R. A., and Surprenant, A. (2001) *EMBO J.* **20,** 6347–6358
44. Grimm, L. M., Goldberg, A. L., Poirier, G. G., Schwartz, L. M., and Osborne, B. A. (1996) *EMBO J.* **15,** 3835–3844
45. Cui, H., Matsui, K., Omura, S., Schauer, S. L., Matulka, R. A., Sonenshein, G. E., and Ju, S. T. (1997) *Proc. Natl. Acad. Sci. U. S. A.* **94,** 7515–7520
46. Hirsch, T., Dallaporta, B., Zamzami, N., Susin, S. A., Ravagnan, L., Marzo, I., Brenner, C., and Kroemer, G. (1998) *J. Immunol.* **161,** 35–40
47. Dallaporta, B., Pablo, M., Maisse, C., Daugas, E., Loeffler, M., Zamzami, N., and Kroemer, G. (2000) *Cell Death Differ* **7,** 368–373
48. Chang, L., and Karin, M. (2001) *Nature* **410,** 37–40
49. Mukherjee, P., and Pasinetti, G. M. (2001) *J. Neurochem.* **77,** 43–49
50. Linford, N. J., Yang, Y., Cook, D. G., and Dorsa, D. M. (2001) *J. Pharmacol. Exp. Ther.* **299,** 67–75
51. Sperandio, S., Poksay, K., de Belle, I., Lafuente, M. J., Liu, B., Nasir, J., and Bredesen, D. E. (2004) *Cell Death Differ* **11,** 1066–1075
52. Werlen, G., Hausmann, B., and Palmer, E. (2000) *Nature* **406,** 422–426
53. Mariathasan, S., Zakarian, A., Bouchard, D., Michie, A. M., Zuniga-Pflucker, J. C., and Ohashi, P. S. (2001) *J. Immunol.* **167,** 4966–4973
54. Budagian, V., Bulanova, E., Brovko, L., Orinska, Z., Fayad, R., Paus, R., and Bulfone-Paus, S. (2003) *J. Biol. Chem.* **278,** 1549–1560
55. Amstrup, J., and Novak, I. (2003) *Biochem. J.* **374,** 51–61
56. Donnelly-Roberts, D. L., Namovic, M. T., Faltynek, C. R., and Jarvis, M. F. (2004) *J. Pharmacol. Exp. Ther.* **308,** 1053–1061
57. Faria, R. X., Defarias, F. P., and Alves, L. A. (2005) *Am. J. Physiol.* **288,** C260–C271
58. Humphreys, B. D., Rice, J., Kertesy, S. B., and Dubyak, G. R. (2000) *J. Biol. Chem.* **275,** 26792–26798
59. Bradford, M. D., and Soltoff, S. P. (2002) *Biochem. J.* **366,** 745–755
60. Suzuki, T., Hide, I., Ido, K., Kohsaka, S., Inoue, K., and Nakata, Y. (2004) *J. Neurosci.* **24,** 1–7
61. Jacques-Silva, M. C., Rodnight, R., Lenz, G., Liao, Z., Kong, Q., Tran, M., Kang, Y., Gonzalez, F. A., Weisman, G. A., and Neary, J. T. (2004) *Br. J. Pharmacol.* **141,** 1106–1117
62. Datta, S. R., Brunet, A., and Greenberg, M. E. (1999) *Genes Dev.* **13,** 2905–2927
63. Duan, S., Anderson, C. M., Keung, E. C., Chen, Y., and Swanson, R. A. (2003) *J. Neurosci.* **23,** 1320–1328
64. Surprenant, A., Rassendren, F., Kawashima, E., North, R. A., and Buell, G. (1996) *Science* **272,** 735–738

A Role for Mitogen-activated Protein Kinase Erk1/2 Activation and Non-selective Pore Formation in P2X7 Receptor-mediated Thymocyte Death

Rodolphe Auger, Iris Motta, Karim Benihoud, David M. Ojcius and Jean M. Kanellopoulos

Access the most updated version of this article at doi: 10.1074/jbc.M501290200

Alerts:
- When this article is cited
- When a correction for this article is posted

Click here to choose from all of JBC's e-mail alerts

This article cites 64 references, 37 of which can be accessed free at
http://www.jbc.org/content/280/30/28142.full.html#ref-list-1